



Efficient aerobic oxidation of biomass-derived 5-hydroxymethylfurfural to 2,5-diformylfuran catalyzed by magnetic nanoparticle supported manganese oxide



Bing Liu^a, Zehui Zhang^{a,*}, Kangle Lv^a, Kejian Deng^a, Hongmin Duan^{b,*}

^a Department of Chemistry, Key Laboratory of Catalysis and Material Sciences of the State Ethnic Affairs Commission & Ministry of Education, South-Central University for Nationalities, Wuhan 430074, China

^b Dalian National Laboratory for Clean Energy, Dalian Institute of Chemical Physics, Chinese Academy of Sciences, 457 Zhongshan Road, Dalian 116023, China

ARTICLE INFO

Article history:

Received 10 September 2013

Received in revised form 2 December 2013

Accepted 10 December 2013

Available online 17 December 2013

Keywords:

Biomass

2,5-Diformylfuran

Aerobic oxidation

5-Hydroxymethylfurfural

Manganese oxide

Magnetic nanoparticles

ABSTRACT

Magnetic Fe_3O_4 supported Mn_3O_4 nanoparticles ($\text{Fe}_3\text{O}_4/\text{Mn}_3\text{O}_4$) were prepared by the solvent thermal method, and its structure was characterized by XRD, XPS, TEM, and FT-IR technologies. The resulting $\text{Fe}_3\text{O}_4/\text{Mn}_3\text{O}_4$ nanoparticles could be used as an excellent heterogeneous catalyst for the aerobic oxidation of the biomass-derived model molecule 5-hydroxymethylfurfural into 2,5-diformylfuran (DFF) under benign reaction conditions. Some important reaction parameters such as reaction temperature, catalyst amount, solvent, oxidant, and oxygen pressure were explored and high DFF yield of 82.1% with HMF conversion of 100% were obtained in DMF under optimal reaction conditions. More importantly, the catalyst could be readily separated from the reaction mixture by a permanent magnet, and recycled up to 6 times without the significant loss of its catalytic activity.

© 2013 Elsevier B.V. All rights reserved.

1. Introduction

At present, we are entering an epoch of diminishing availability of petrochemical resources, which are mainly used to produce chemical products and energy for our society. The limited oil resources render the current petroleum based fuel and chemical production schemes unsustainable. Thus, much effort has been devoted to explore the renewable feedstocks to meet the increasing demand for fuels and chemicals [1]. Biomass as the only carbon-containing renewable resource has received considerable attention as an alternative feedstock for the production of fuels and chemicals [2–4]. Carbohydrates are the major component of biomass feedstock. The biopolymers such as cellulose and hemi-cellulose are readily available from various biomass sources. From those, monosaccharides are obtained by the depolymerization of the biopolymers, which can be further converted into various chemicals and liquids fuels [5–7].

5-Hydroxymethylfurfural (HMF), the acid-catalyzed dehydration product of C6 based carbohydrates, is considered to be a

versatile platform chemical. It can be used as a precursor for the synthesis of fine chemicals, pharmaceuticals, polymers and liquids fuels [8]. In this context, various methods have been developed for the synthesis of HMF from carbohydrates [9–13].

Recently, 2,5-diformylfuran (DFF), which is one of the oxidation products of HMF, has attracted much attention. It can not only be used to as a monomer for the production multifunctional materials [14,15], but also as the starting material for the synthesis of drugs, antifungal agents, nematocides, and ligands [16,17]. However, it is challenging for the selective oxidation of HMF into DFF, as various oxidation products can be produced such as 5-formyl-2-furancarboxylic acid (FFCA), 5-hydroxymethyl-2-furancarboxylic acid (HMFC), and 2,5-furandicarboxylic acid (FDCA). Synthesis of DFF has been early reported from the oxidation of HMF using traditional oxidants such as NaOCl [18], BaMnO_4 [19], and pyridinium chlorochromat [20]. These methods not only required stoichiometric oxidants, but also released serious toxicity wastes. Therefore, it is strongly demanded to develop environmentally friendly systems for the selective oxidation of HMF into DFF.

Recently, there is a growing attention in the synthesis of DFF from the oxidation of HMF with molecular oxygen catalyzed by heterogeneous catalysts. The supported Ru based catalysts generally showed high HMF conversion and DFF selectivity [21–24], but some required high pressure. The vanadium-based catalysts also

* Corresponding authors. Tel.: +86 27 67842752; fax: +86 27 67842752.

E-mail addresses: zehuizh@mail.ustc.edu.cn (Z. Zhang), dhm@dicp.ac.cn (H. Duan).

have been attracted much attention for the aerobic oxidation of HMF into DFF [25,26], but some vanadium-based catalyst easily lost its catalytic activity. Furthermore, the catalyst recycling procedures using filtration and centrifugation were tedious, which inevitably leads to the loss of catalyst in the separation processes. Therefore, the development of new catalytic systems for the oxidation of HMF into DFF is strongly demanded. Recently, magnetic materials based heterogeneous catalysts have received growing attention due to their unique properties [27]. Magnetic separation is a convenient method for catalyst recycling, which overcomes the disadvantages caused by the traditional separation method.

Due to the high price of noble metals, innovating cheap transition metal-based heterogeneous catalysts for the synthesis of DFF from the oxidation of HMF is thus highly desirable. In the past decade, some methods on the aerobic oxidation of alcohols using relative cheap Mn based catalysts were reported [28]. Inspired by the excellent catalytic activity of Mn_3O_4 nanoparticles in the aerobic oxidation of alcohols and the unique property of magnetic catalysts, herein, we developed a new method for the synthesis of magnetic Fe_3O_4 supported Mn_3O_4 nanoparticles ($\text{Fe}_3\text{O}_4/\text{Mn}_3\text{O}_4$), and used as a novel heterogeneous catalyst for the aerobic oxidation of HMF into DFF. To the best of our knowledge, this is the first report on the aerobic oxidation of HMF into DFF catalyzed by magnetic $\text{Fe}_3\text{O}_4/\text{Mn}_3\text{O}_4$ nanoparticles.

2. Experimental

2.1. Materials and methods

Fe_3O_4 nanoparticles were prepared and characterized as described in our previous work [29]. $\text{Mn}(\text{OAc})_2 \cdot 4\text{H}_2\text{O}$ and hexadecyl trimethyl ammonium bromide (CTAB) were purchased from Sinopharm Chemical Reagent Co., Ltd. (Shanghai, China). 5-Hydroxymethylfurfural (98%) was purchased from Aladdin Chemicals Co., Ltd. (Beijing, China). 2,5-Diformylfuran (DFF) was purchased from J&K Co., Ltd. (Beijing, China). Acetonitrile (HPLC grade) was purchased from Tedia Co. (Fairfield, USA). All other reagents were provided by local supplies (Wuhan, China). All the solvents were purchased from Sinopharm Chemical Reagent Co., Ltd. (Shanghai, China) and freshly distilled before use.

2.2. Preparation of Mn_3O_4 nanoparticles

Mn_3O_4 nanoparticles were prepared according to the known procedures [30]. $\text{Mn}(\text{OAc})_2 \cdot 4\text{H}_2\text{O}$ (0.50 g) was firstly dissolved in dimethyl sulfoxide (DMSO) (30 mL) with sonication-assist. This solution was then transferred into a 100 mL Teflon-lined stainless steel autoclave and heated at 120 °C for 6.5 h. After the slow cooling to room temperature, water (30 mL) was added into the mixture, and the black Mn_3O_4 nanoparticles were precipitated after keeping it at room temperature for 2 h. The black Mn_3O_4 nanoparticles were thoroughly washed with deionized water and ethanol several times, separated by centrifugation, then dried at 60 °C for 6 h in vacuum.

2.3. Preparation of the catalyst $\text{Fe}_3\text{O}_4/\text{Mn}_3\text{O}_4$

$\text{Mn}(\text{OAc})_2 \cdot 4\text{H}_2\text{O}$ (0.50 g) and CTAB (30 mg) were firstly dissolved in DMSO (50 mL) in a 100 mL Teflon-lined stainless steel autoclave. Then Fe_3O_4 (0.10 g) was dispersed into the above solution with sonication-assist for 30 min. Then the autoclave was sealed, and it was heated at 120 °C for 6.5 h. Other steps were the same as described above for the synthesis of Mn_3O_4 .

2.4. Catalyst characterization

Transmission electron microscope (TEM) images were obtained using an FEI Tecnai G²-20 instrument. The sample powder were firstly dispersed in ethanol and dropped onto copper grids for observation. FT-IR measurements were recorded on a Nicolet NEXUS-6700 FTIR spectrometer with a spectral resolution of 4 cm⁻¹ in the wave number range of 500–4000 cm⁻¹. X-ray powder diffraction patterns of samples were determined with a Bruker advanced D8 powder diffractometer (Cu K α). The scan ranges were 10–80° with 0.016° steps, respectively. X-ray photoelectron spectroscopy (XPS) was conducted on a Thermo VG scientific ESCA MultiLab-2000 spectrometer with a monochromatized Al K α source (1486.6 eV) at constant analyzer pass energy of 25 eV. The binding energy was estimated to be accurate within 0.2 eV. All binding energies (BEs) were corrected referencing to the C1s (284.6 eV) peak of the contamination carbon as an internal standard.

2.5. Aerobic oxidation of HMF under atmospheric pressure

The aerobic oxidation of HMF under atmospheric pressure was carried out in a 25 mL round bottom flask, which was coupled with a reflux condenser and capped with a balloon. Typically, HMF (1 mmol, 126 mg) was firstly dissolved into DMF (7 mL) with a magnetic stirrer. Then, the catalyst $\text{Fe}_3\text{O}_4/\text{Mn}_3\text{O}_4$ was added into the reaction mixture and flushed with pure oxygen at a rate of 20 mL min⁻¹. The reaction was carried out at 110 °C for the desired reaction time. Time zero was taken when the oxygen was flushed into the reaction mixture. After reaction, the catalyst $\text{Fe}_3\text{O}_4/\text{Mn}_3\text{O}_4$ was separated from the reaction mixture by a permanent magnet, and the products were analyzed by HPLC method.

2.6. Aerobic oxidation of HMF under high pressure

Aerobic oxidation of HMF under high pressure was carried out in semi-batch reactor. Briefly, HMF was firstly dissolved in DMF, and then the catalyst was added into the reactor. The reactor was subsequently sealed and oxygen was charged to the desired pressure. Then the temperature was adjusted to the chosen value and the reaction was allowed to proceed with a magnetic stirring at 600 rpm. After a predetermined reaction time, the reaction was stopped by cooling the reactor with tap water to room temperature. The gas in the reactor was slowly released and the reaction liquid was analyzed by HPLC method.

2.7. Determination of the products

HMF and DFF were quantified by HPLC system using external standard calibration curve method. Samples were separated by a reversed-phase C18 column (200 mm × 4.6 mm) at a wavelength of 280 nm. Acetonitrile and 0.1 wt.% acetic acid aqueous solution, volume ratio 15:85, were used as the mobile phase, and the samples were eluted at a rate of 1.0 mL min⁻¹ at 25 °C. The content of HMF and DFF in samples were obtained directly by interpolation from calibration curves, which were constructed based on the pure compounds.

To calculate the yield of DFF from HMF equation (1) was used

$$\text{HMF conversion} = \frac{\text{Moles of HMF added} - \text{Moles of unreacted HMF}}{\text{Moles of HMF added}} \times 100\% \quad (1)$$

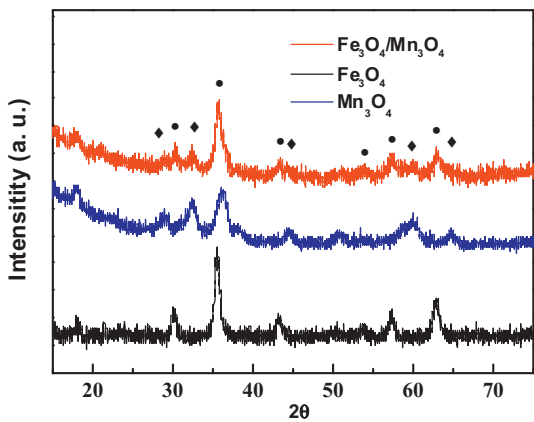


Fig. 1. XRD patterns of the samples. The circle represents Fe_3O_4 , and the rhombus represents Mn_3O_4 .

One molecule of HMF gave rise to one molecule DFF. DFF yield can be calculated using Eq. (2)

$$\text{DFF yield} = \frac{\text{Moles of DFF}}{\text{Moles of HMF added}} \times 100\% \quad (2)$$

2.8. Catalyst recycling

After reaction, the catalyst $\text{Fe}_3\text{O}_4/\text{Mn}_3\text{O}_4$ was separated from the reaction mixture by a permanent magnet, and washed three times with water and ethanol, dried at 60°C over night in a vacuum oven. Then the recovered catalyst was used for the second cycle under the same conditions, which were used for the first time. These processes were repeated for five times to test the stability of the catalyst.

3. Results and discussion

3.1. Synthesis and characterization of catalyst

The schematic illustration for the synthesis of $\text{Fe}_3\text{O}_4/\text{Mn}_3\text{O}_4$ catalyst is shown in Fig. S1. The magnetic Fe_3O_4 nanoparticles used as the support were prepared via co-precipitation of an aqueous mixture of ferric and ferrous salts under a strong alkaline solution [29]. According to the previous results [30], the sulfur atom in DMSO had so-called lone pair electrons, which captured the H^+ in H_2O . Thus, a lot of OH^- were released from H_2O in the presence of lone pair electrons in DMSO, which accelerated the formation of coordination compounds $[\text{Mn}(\text{OH})_x(\text{DMSO})_{6-x}]^{2-x}$ (Fig. S1). $[\text{Mn}(\text{OH})_x(\text{DMSO})_{6-x}]^{2-x}$ species were not stable at high temperature, being decomposed into tiny and large quantities of $\text{Mn}(\text{OH})_2$ crystal nuclei. Then $\text{Mn}(\text{OH})_2$ nuclei was further oxidized by O_2 in ambient environment into hausmannite Mn_3O_4 , which was the most stable phase of manganese oxide. The formed Mn_3O_4 nanoparticles were then deposited on the dispersed Fe_3O_4 nanoparticles to give rise to the magnetic $\text{Fe}_3\text{O}_4/\text{Mn}_3\text{O}_4$ nanoparticles.

Fig. 1 shows the XRD patterns of Fe_3O_4 , Mn_3O_4 and $\text{Fe}_3\text{O}_4/\text{Mn}_3\text{O}_4$. All the peaks of Mn_3O_4 could be assigned to the tetragonal cell structure of Mn_3O_4 , which were consistent with those of tetragonal phase (JCPDS Card No. 18-0803) [31]. An intense peak at $2\theta = 36.1^\circ$ was observed in the XRD pattern of Mn_3O_4 , which was corresponded to (2 1 1) plane of Mn_3O_4 . Other peaks with low intensity were also matched well with those reported in JCPDS Card (18-0803). All the diffraction peaks of Fe_3O_4 should be assigned to the planes of inverse cubic spinel structured Fe_3O_4 , which was consistent with the standard Fe_3O_4 sample (JCPDS File No. 19-0629).

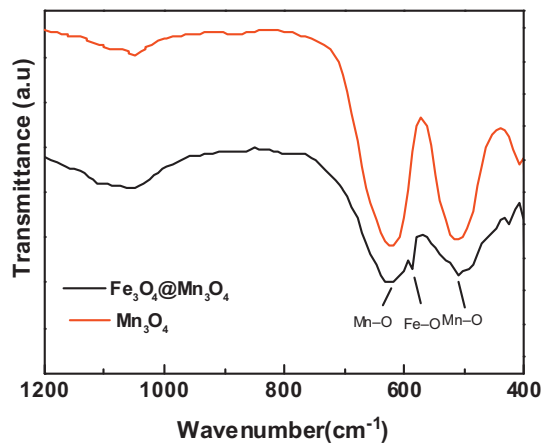


Fig. 2. FT-IR spectra of the samples.

[32]. Particularly, a strong peak at $2\theta = 35.5^\circ$ was observed in the XRD pattern of Fe_3O_4 sample. The XRD pattern of $\text{Fe}_3\text{O}_4/\text{Mn}_3\text{O}_4$ was also collected, and a strong peak at $2\theta = 35.7^\circ$ was observed. Compared the XRD patterns of $\text{Fe}_3\text{O}_4/\text{Mn}_3\text{O}_4$ with those of Mn_3O_4 and Fe_3O_4 , the strong peak at $2\theta = 35.7^\circ$ in $\text{Fe}_3\text{O}_4/\text{Mn}_3\text{O}_4$ is different from those of Fe_3O_4 at $2\theta = 35.5^\circ$ and Mn_3O_4 at $2\theta = 36.1^\circ$. The reason might be that it was the overlap of the peak of Fe_3O_4 at $2\theta = 35.5^\circ$ and the peak of Mn_3O_4 at $2\theta = 36.1^\circ$. In addition, some peaks with low intensity were also appeared in $\text{Fe}_3\text{O}_4/\text{Mn}_3\text{O}_4$, and all the peaks could be assigned to the corresponding peaks either in Fe_3O_4 or Mn_3O_4 . These XRD results confirmed that the catalyst $\text{Fe}_3\text{O}_4/\text{Mn}_3\text{O}_4$ was composed of Fe_3O_4 and Mn_3O_4 .

As shown in Fig. 2, two bands at 621 cm^{-1} and 513 cm^{-1} were assigned to the Mn–O stretching modes in tetrahedral sites and the distortion vibration of Mn–O in an octahedral environment, respectively [33]. A weak band at 410 cm^{-1} was attributed to the vibration of manganese species (Mn^{3+}) in an octahedral site. Compared the FT-IR spectra of $\text{Fe}_3\text{O}_4/\text{Mn}_3\text{O}_4$ with that obtained from Mn_3O_4 , a new peak at 583 cm^{-1} was appeared in $\text{Fe}_3\text{O}_4/\text{Mn}_3\text{O}_4$. The peak at 583 cm^{-1} was the characteristic peak of Fe_3O_4 , which was the vibration of Fe–O bond [34]. The FT-IR results also indicated that Mn_3O_4 was successfully supported on the magnetic Fe_3O_4 nanoparticles.

Fig. 3 shows the representative TEM images of Mn_3O_4 and $\text{Fe}_3\text{O}_4/\text{Mn}_3\text{O}_4$. As shown in Fig. 3(a), most of Mn_3O_4 nanoparticles showed spherical morphology and uniform size distribution with the diameter in 5–6 nm. Compared the TEM image of $\text{Fe}_3\text{O}_4/\text{Mn}_3\text{O}_4$ with that of Mn_3O_4 , $\text{Fe}_3\text{O}_4/\text{Mn}_3\text{O}_4$ was also observed with spherical shape, but some slight aggregation was observed in $\text{Fe}_3\text{O}_4/\text{Mn}_3\text{O}_4$. As the density and the color of Fe_3O_4 are close to Mn_3O_4 , it was difficult to discriminate Fe_3O_4 and Mn_3O_4 in the sample of $\text{Fe}_3\text{O}_4/\text{Mn}_3\text{O}_4$. Therefore, the catalyst $\text{Fe}_3\text{O}_4/\text{Mn}_3\text{O}_4$ was further characterized by the energy-dispersive analysis of X-ray (EDAX). The results obtained from EDAX provided the information that the catalyst $\text{Fe}_3\text{O}_4/\text{Mn}_3\text{O}_4$ was composed of O, Fe, and Mn elements (Fig. S2). The ratio of Mn wt.% to Fe wt.% from the EDAX elemental analysis is 1.87.

The surface of Mn_3O_4 and $\text{Fe}_3\text{O}_4/\text{Mn}_3\text{O}_4$ was further characterized by XPS (Fig. 4 and Fig. S3). All the measurements were carried out with reference to the C1s binding energy (284.6 eV) as an internal standard. A Mn 2p_{3/2}–2p_{1/2} doublet at 653.7 eV and 642.9 eV is observed for Mn_3O_4 in Fig. 4(a), and the splitting width (11.8 eV) is consistent well with the earlier reports [35]. Compared the XPS spectra of Mn_3O_4 with that of $\text{Fe}_3\text{O}_4/\text{Mn}_3\text{O}_4$ (Fig. S3), two new peaks with the binding energy (BE) values at 711.1 eV and 724.6 eV were only existed in $\text{Fe}_3\text{O}_4/\text{Mn}_3\text{O}_4$. The peaks at 711.1 eV and 724.6 eV were attributed to the binding energy of Fe 2p_{3/2} and

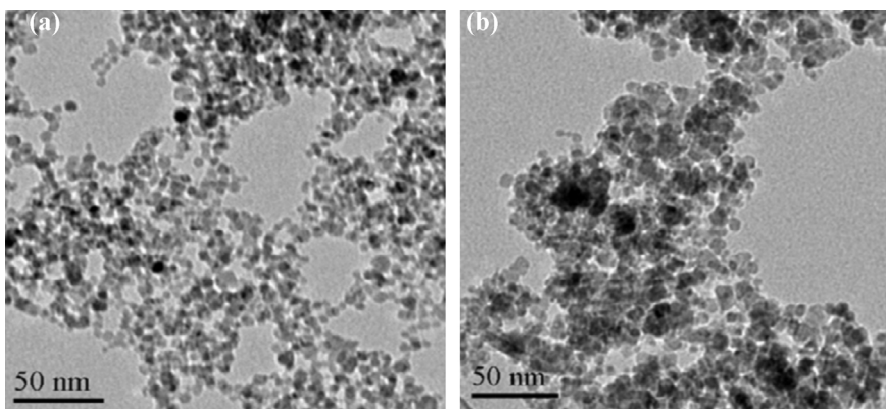


Fig. 3. TEM image of the samples. (a) Mn₃O₄; (b) Fe₃O₄/Mn₃O₄.

Fe 2p1/2, respectively, Fig. 4(b), which was the characteristic of Fe²⁺ in Fe₃O₄ [36]. From the XPS results, it was clearly confirmed that the catalyst Fe₃O₄/Mn₃O₄ was composed of Fe₃O₄ and Mn₃O₄. The ratio of Mn wt.% to Fe wt.% determined by XPS analysis was 2.82, which was much higher than that obtained by EDX analysis. As EDAX provided the whole elemental analysis, and XPS analysis

provided mainly the surface elemental analysis. The result of XPS was much higher than that obtained by EDX, indicating that most Mn₃O₄ particle supported on the Fe₃O₄ surface.

3.2. Synthesis of DFF from HMF under various conditions

The stability of HMF was firstly studied. HMF was stable in DMF without catalyst and the flush of oxygen, and it was recovered by 95.7% in DMF for 4 h at 120 °C (Table 1, Entry 1). The results indicated that HMF itself was stable in DMF under neutral conditions, which was consistent with the previous results [37]. Under acidic conditions, the acid-catalyzed side reactions such as aldol addition and condensation were present [38]. Under alkaline conditions, some side reactions such as condensation and cannizarro reactions occurred [39]. Thus the neutral reaction condition was an important safeguard to achieve high DFF yield and selectivity.

Mn₃O₄ nanoparticles showed high catalytic activity on the aerobic oxidation of HMF into DFF, which produced DFF in a high yield of 83.2% with HMF conversion of 100% (Table 1, Entry 2). To our pleasure, the magnetic Fe₃O₄/Mn₃O₄ catalyst also showed high catalytic activity, and DFF yield of 82.1% was obtained, which was close to that obtained with Mn₃O₄ as the catalyst (Table 1, Entries 2 vs 3). As a blank experiment, the support Fe₃O₄ was ineffective for the aerobic oxidation of HMF (Table 1, Entry 4). These results indicated that Mn₃O₄ nanoparticles were the active sites of Fe₃O₄/Mn₃O₄ in the aerobic oxidation of HMF. Unlike the prepared Mn₃O₄ nanoparticles, the commercial available manganese oxides such as Mn₂O₃ and MnO₂ gave poor catalytic performance (Table 1, Entries 5–7). Specifically, the catalytic activity of the commercial Mn₃O₄ was much lower than that of the prepared Mn₃O₄ nanoparticles (Table 1, Entries 2 vs 7). As the BET surface area of our prepared Mn₃O₄ nanoparticles and the commercial Mn₃O₄ were determined to be 86.7 and 7 m²/g, respectively, the higher catalytic activity of the prepared Mn₃O₄ was mainly due to the high surface area, which could provide a large number of active sites. In addition, poor results were also obtained when homogeneous manganese salts such as MnCl₂·4H₂O and Mn(OAc)₂·4H₂O were used as the catalysts (Table 1, Entries 8 and 9).

3.3. Effect of the solvents on the aerobic oxidation of HMF

The aerobic oxidation of HMF was further carried out in a variety of solvents. As shown in Table 2, the solvent showed a remarkable effect on the oxidation of HMF. DMSO and DMF with strong polarity and high boiling point were found to be the best solvents. HMF conversions reached 83.5% and 84.5% with DMSO and DMF, respectively (Table 2, Entries 1 and 2). However, the selectivity of

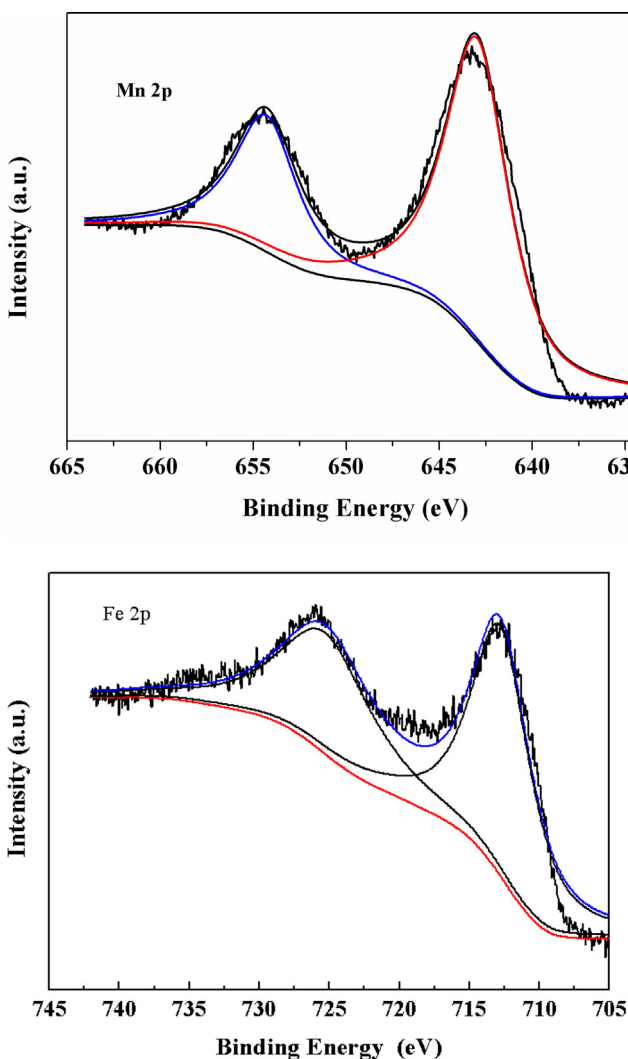


Fig. 4. XPS spectra of Fe₃O₄/Mn₃O₄. (a) Mn 2p region; (b) Fe 2p.

Table 1Catalytic conversion of HMF into DFF under various conditions.^a

Entry	Catalyst	Catalyst amount (mg)	Time (h)	HMF conversion (%)	DFF yield (%)
1 ^b	–	–	4	4.3	0
2 ^c	Mn ₃ O ₄	108	4	100	83.2
3	Fe ₃ O ₄ /Mn ₃ O ₄	160	4	99.8	82.1
4	Fe ₃ O ₄	108	12	5.9	0.4
5	Mn ₂ O ₃	112	12	7.7	2.3
6	MnO ₂	123	12	6.5	0.6
7 ^d	Mn ₃ O ₄	108	12	23.4	17.8
8	Mn(OAc) ₂ ·4H ₂ O	346	12	11.5	9.0
9	MnCl ₂ ·4H ₂ O	280	12	7.1	3.5

^a Reaction conditions: HMF (126 mg, 1 mmol) and a set amount of catalyst were added into DMF (7 mL), and the reaction was carried out at 120 °C with the flush of molecular oxygen at a rate of 20 mL min⁻¹.

^b The reaction was carried out without catalyst and molecular oxygen.

^c The catalyst was the prepared Mn₃O₄ nanoparticles.

^d The catalyst was the commercial Mn₃O₄.

DFF in DMF was much higher than that in DMSO, as much more DFF was further oxidized into FDCA in DMSO. Moderate HMF conversions around 40% were obtained in tetrahydrofuran (THF) and toluene (Table 2, Entries 3 and 4), but the selectivity of DFF in THF was the lowest of all testing solvents. Reactions carried in other solvents MIBK (methyl isobutyl ketone), MeCN and CHCl₃ produced low HMF conversion (Table 2, Entries 5–7). These results indicated that DMF was a superior solvent for the aerobic oxidation of HMF into DFF. According to the results reported by Biswal et al., we speculated that Mn³⁺ was the active site for oxidation of HMF. According to the general acceptable mechanism of oxidation of HMF and alcohols [40], the active center Mn³⁺ was reduced to Mn²⁺ by the abstraction of one hydrogen atom connected with carbon atom in –CH₂OH group, and simultaneously produced the carbon cation, which then released H⁺ to give rise to DFF. Then the oxygen was reoxidized Mn²⁺ to Mn³⁺, which generated the catalytic cycle.

Based on the general knowledge of solvent effect, the strong polar solvents such as DMSO and DMF are beneficial to stabilize the positive charge of the cations. Thus, high DFF yield was obtained when the aerobic oxidation of HMF catalyzed by Fe₃O₄/Mn₃O₄ was carried out in DMF.

3.4. Effect of catalyst amount the aerobic oxidation of HMF

The aerobic oxidation of HMF was also carried out with various amounts of Fe₃O₄/Mn₃O₄ in order to study the effect of the catalyst loading. As shown in Table 3, the loading of Fe₃O₄/Mn₃O₄ showed a remarkable effect on the aerobic oxidation of HMF. HMF conversions were 27.1% and 43.9% after 12 h with 40 mg and 80 mg of Fe₃O₄/Mn₃O₄, respectively, and the corresponding DFF yields were 22.2% and 37.5% (Table 3, Entries 1 and 2). HMF conversions reached 84.5% and 100% for 6 h and 10 h, respectively, when 120 mg

of Fe₃O₄/Mn₃O₄ was used (Table 3, Entries 3 and 4). Further increasing the amount of Fe₃O₄/Mn₃O₄ to 160 mg, the aerobic oxidation of HMF proceeded fast (Table 3, Entries 5 and 6). It only required 4 h to obtain the maximum DFF yield of 82.1% with HMF conversion of 100% (Table 3, Entry 6). The higher the catalyst amount was, the higher the HMF conversion and DFF yield were at the same reaction time. It should be attributed to an increase in the availability and number of catalytically active sites, and a similar phenomenon was also observed for the oxidation of benzyl alcohol [41]. However, it was noted that the selectivity of DFF was almost the same around 80–85% with various catalyst loadings. These results indicated that the selectivity of DFF had no relationship with the catalyst loading when the reactions were carried out under otherwise the same reaction conditions such as reaction temperature, and solvent. Compared our method with the aerobic oxidation of HMF with K-OMS-2 (KMn₈O₁₆·nH₂O) reported by Yang et al. [42], our method produced a lower HMF yield than that catalyzed by K-OMS-2. The main reason was mainly caused by the catalyst itself. Our catalyst showed lower selectivity as 11.5% FDCA was also formed. However, the great advantage of our newly developed method was that the catalyst could be readily removed from the reaction mixture by an external magnet.

3.5. Oxidation of HMF using various oxidants

The influence of oxygen pressure on the aerobic oxidation of HMF was also studied. Reactions were carried out in autoclave reactor with the oxygen pressure at 5 bar, 10 bar, and 15 bar with 40 mg of the catalyst, respectively. As shown in Table 4, higher pressure promoted higher HMF conversion and DFF yield (Table 4, Entries 1–4). The reason was that the oxygen concentration in DMF became higher with the increase of oxygen pressure, thus HMF conversion became higher with the increase of oxygen pressure at the same reaction time period. However, the effect of oxygen pressure on the catalytic activity of Fe₃O₄/Mn₃O₄ was not very remarkable with 40 mg of Fe₃O₄/Mn₃O₄. Sádaba et al. [26] also found that HMF conversion in DMSO increased with the increase of oxygen pressure, but it was also not distinct, in which HMF conversions were 84% and 91% with 2.5 bar and 10 bar oxygen under otherwise the same conditions.

In addition, the effect of the oxygen pressure on the aerobic oxidation of HMF was also studied with the use of 160 mg of Fe₃O₄/Mn₃O₄. A similar trend was also observed for the use of 160 mg of Fe₃O₄/Mn₃O₄ (Table 3, Entry 5 and Table 4, Entries 6 and 7). Other oxidants such as H₂O₂ and t-BuOOH were also used for the oxidation of HMF. Among these oxidants, the clean and cheap oxidant O₂ was found to be the best oxidant (Table 4, Entry 5). Although t-BuOOH has been used as a common oxidant in the oxidation of organic compounds, it was ineffective for the oxidation of HMF.

Table 2Effect of the solvents on the aerobic oxidation of HMF into DFF.^a

Entry	Solvent	HMF conversion (%)	DFF yield (%)	DFF selectivity (%)	FDCA yield (%)
1	DMSO	83.5	50.7	60.7	27.8
2	DMF	84.5	71.8	84.9	7.9
3	THF	39.8	17.6	44.2	15.0
4	Toluene	43.2	30.1	69.7	9.1
5	MIBK	17.8	11.4	64.0	4.0
6	MeCN	9.1	5.8	63.7	1.9
7	CHCl ₃	19.7	12.5	63.4	4.1

^a Reaction conditions: HMF (126 mg, 1 mmol) and Fe₃O₄/Mn₃O₄ (120 mg) were added into the solvent (7 mL), and the reaction was carried out at 120 °C for 6 h with the flush of molecular oxygen at a speed of 20 mL min⁻¹.

Table 3Effect of catalyst loading on the aerobic oxidation of HMF into DFF.^a

Entry	Catalyst amount (mg)	Time (h)	HMF conversion (%)	DFF yield (%)	DFF selectivity (%)	FDCA yield (%)
1	40	12	27.1	23.2	85.6	3.2
2	80	12	43.9	37.5	85.4	4.9
3	120	6	84.5	71.8	84.9	7.9
4	120	10	100	80.9	80.9	12.8
5	160	2	81.3	69.7	85.7	9.4
6	160	4	100	82.1	82.1	11.5

^a Reaction conditions: HMF (126 mg, 1 mmol) and a set amount of Fe₃O₄/Mn₃O₄ were added into DMF (7 mL), and the reaction was carried out at 120 °C with the flush of molecular oxygen at a speed of 20 mL min⁻¹.

HMF conversion reached 84.2% using *t*-BuOOH as oxidant, but the selectivities of DFF and FDCA were both low (Table 4, Entry 8). Other oxidation furan compounds such as HMFCA also did not formed. The reason was that the furan ring was destroyed by the strong oxidative ability of *t*-BuOOH. Both the HMF conversion and DFF yield were very low when H₂O₂ was used as the oxidant (Table 4, Entry 9). It was reported that the manganese oxide such as MnO₂, Mn₅O₈ and Mn₃O₄ could catalyze the decomposition of H₂O₂ [43]. It was observed a severe reaction between the catalyst and H₂O₂ at the start of the addition of H₂O₂ that was caused by H₂O₂ decomposition and, consequently, the oxidation of HMF did not occur sufficiently.

3.6. Time course of the aerobic oxidation of HMF into DFF at different reaction temperatures

Finally, the aerobic oxidation of HMF was carried out at 80 °C, 100 °C, and 120 °C, respectively, with the aim to study the effect of reaction temperature. As shown in Fig. 5, HMF conversion and DFF yield increased with the increase of reaction temperature at the same reaction time points. Taking the reaction time of 2 h as an example, HMF conversions reached 19.6%, 30.6% and 81.3% at 80 °C, 100 °C and 120 °C, respectively, and the corresponding DFF yields were 16.7%, 28.4%, and 69.7%, respectively. It only required 4 h to obtain the highest DFF yield of 82.1% with HMF conversion of 100% at 120 °C. Interestingly, DFF was stable under the reaction conditions, as DFF yield slightly decreased from 82.1% at 4 h to 77.0% at 12 h. HMF conversion and DFF yield gradually increased at 80 °C and 100 °C during the reaction process. HMF conversions reached 49.9% and 87.5% after 12 h at 80 °C and 100 °C, respectively, and the corresponding DFF yields were 40.6% and 80.2%, respectively. These results indicated that high reaction temperature promoted the aerobic oxidation of HMF into DFF. Our results were consistent with the previous results reported by Antonyraj et al. [23], in which they found that the aerobic conversion of HMF catalyzed

by Ru/γ-alumina gradually increased with the increase of reaction temperature in the range from 80 °C to 130 °C.

3.7. Catalyst recycling experiments

The catalyst recycling experiments were investigated with goal of green chemistry, and the aerobic oxidation of HMF into DFF was used as a model reaction. Reactions were carried out in DMF at 120 °C. After reaction, the Fe₃O₄/Mn₃O₄ catalyst was dispersed in the reaction mixture, and the reaction mixture was muddy (Fig. S4(a)). But the catalyst Fe₃O₄/Mn₃O₄ could be fast separated from the reaction mixture by a permanent magnet (Fig. S4(b)). Then the recovered catalyst was washed three times with water and ethanol, dried at 80 °C over night in a vacuum oven. Then the recovered catalyst was used for the second cycle under the same conditions. These processes were repeated for five times to test the stability of the catalyst. As shown in Fig. 6, DFF yields remained stable during the recycling experiments (82.1% in first cycle vs 78.9% in sixth cycle). The spent catalyst after the sixth cycle was characterized by XRD. It was found that there was no difference in the XRD patterns between the fresh catalyst and the spent catalyst (Fig. S5). Thus the most possible reason for the slight decrease of the catalytic activity was due to the inevitable loss of the catalyst mass during the recycling procedures.

3.8. Comparison our method with other reported methods for the oxidation of HMF

In order to give a reasonable evaluation of our developed method for the synthesis of DFF from HMF, the developed method was compared with other recently reported methods, and the results are shown in Table 5. The noble metal Ru based catalysts generally showed high HMF conversion and DFF selectivity (Table 5, Entries 1–3), but some cases required high pressure (Table 5, Entries 1 and 2), which was potentially dangerous in practical application.

Table 4Catalytic oxidation of HMF using various oxidants.^a

Entry	Oxidant	Catalyst amount (mg)	Time (h)	HMF conversion (%)	DFF yield (%)	FDCA yield (%)
1 ^b	O ₂	40	12	27.1	22.2	3.2
2 ^c	O ₂	40	12	35.5	29.8	2.6
3 ^d	O ₂	40	12	53.1	41.9	6.3
4 ^e	O ₂	40	12	60.8	45.1	7.8
5 ^b	O ₂	160	4	100	82.1	11.5
6 ^c	O ₂	160	2	95.4	80.3	10.1
7 ^d	O ₂	160	2	100	79.4	12.8
8 ^f	<i>t</i> -BuOOH	160	4	84.2	7.2	5.6
9 ^g	H ₂ O ₂	160	4	13.2	5.3	3.6

^a Reaction conditions: HMF (126 mg, 1 mmol) and a set amount of Fe₃O₄/Mn₃O₄ were added into DMF (7 mL), and the reaction was carried out at 120 °C using various oxidant.

^b 1 bar with the flush of oxygen at 20 mL min⁻¹.

^c 5 bar oxygen.

^d 10 bar oxygen.

^e 15 bar oxygen.

^f 7 mmol of *t*-BuOOH was used.

^g 7 mmol of H₂O₂ was used.

Table 5

Catalytic oxidation of HMF into DFF using various methods.

Entry	Catalyst	Reaction conditions	HMF conversion (%)	DFF yield (%)	References
1	Ru/C	383 K, 2.0 MPa O ₂	100	96.0	[21,22]
2	Ru/ γ -alumina	403 K, 40 pis O ₂	100	97.0	[23]
3	Ru/Hydrotalcite	393 K, 1 bar O ₂ at 20 mL/min	94.8	92.0	[24]
4	VO ²⁺ /Cu ²⁺ -immobilized on sulfonated carbon catalyst	413 K, 40 bar Ar	100	98.0	[25]
5	V ₂ O ₅ /H-beta	398 K, 40 bar O ₂	92	81	[26]
6	Porphyrin-based polymer-supported iron(III)	383 K, 5 bar O ₂	63	31	[44]
7	Fe ₃ O ₄ /Mn ₃ O ₄	393 K, 1 bar O ₂ at 20 mL min ⁻¹	100	82.1	This work

In addition, the high cost of Ru made those catalysts less attractive. Recently, the non-noble catalysts have been attracted much attention. The vanadium based catalysts seemed to be promising in the aerobic oxidation of HMF. However, these catalytic systems also had some distinct drawbacks such as the requirement of high pressure, the need of co-catalyst (Table 5, Entry 4) and the loss of catalytic activity (Table 5, Entry 5). Recently, the porphyrin-based polymer-supported iron(III) was also used for the oxidation of HMF, but low HMF conversion and low DFF selectivity were obtained (Table 5, Entry 6). Albeit our developed Fe₃O₄/Mn₃O₄ catalytic system showed a little lower DFF selectivity as compared with some of the mentioned methods, it demonstrated some unique advantages (Table 5, Entry 7). Firstly, the recovery of Fe₃O₄/Mn₃O₄ was convenient with the assist of an external magnet. Secondly, the cost was

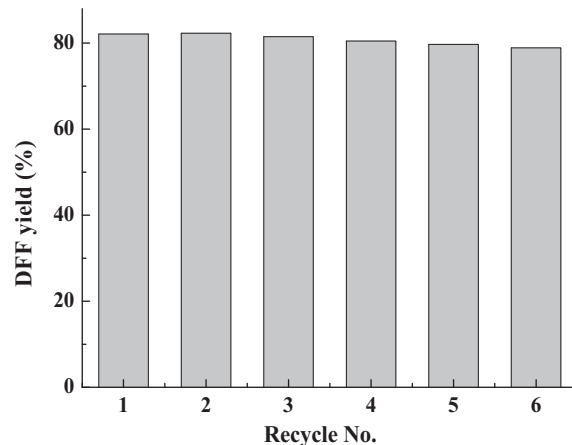


Fig. 6. Recycle experiments of the catalyst Fe₃O₄/Mn₃O₄. Reaction conditions: HMF (126 mg, 1 mmol) and Fe₃O₄/Mn₃O₄ (160 mg) were added into 7 mL of DMF, then the reaction was carried out at 120 °C with the flush of dioxygen at a speed of 20 mL min⁻¹.

much lower in comparison with the tradition noble metal catalysts, which undoubtedly saved the cost in the practical application.

4. Conclusion

In conclusion, a new method was developed for the synthesis of DFF from the aerobic oxidation of HMF into DFF. The magnetic Fe₃O₄/Mn₃O₄ catalyst showed an excellent catalytic performance with DFF yield of 82.1%. The catalyst could be readily separated from the reaction mixture by a permanent magnet, and could be reused for several times without the loss of its catalytic activity. The high activity, stability, magnetic recyclability, combining the facile preparation of the catalyst make them promising applications in conversion of biomass derived platform chemicals into valuable bulk chemicals.

Acknowledgements

This project was supported by National Natural Science Foundation of China (Nos. 21203252, 21206200).

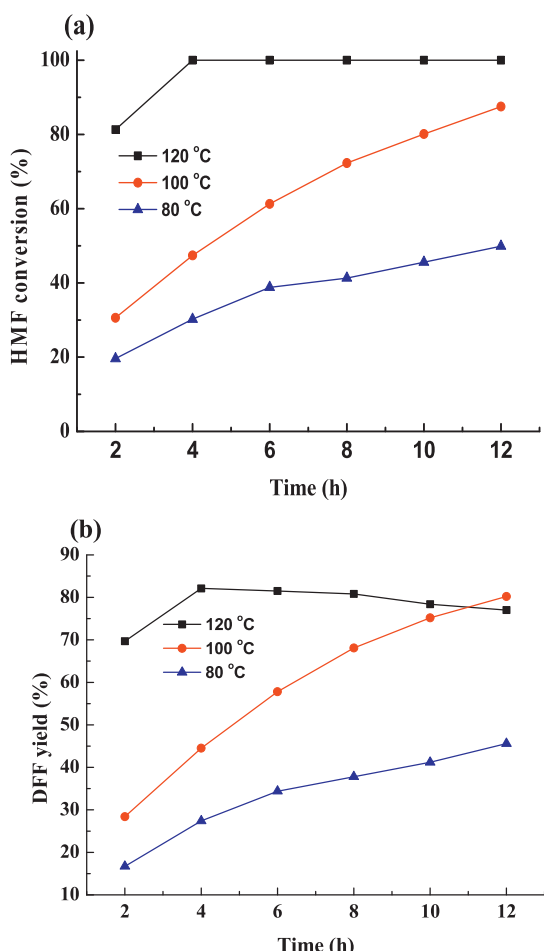
Appendix A. Supplementary data

Supplementary data associated with this article can be found, in the online version, at <http://dx.doi.org/10.1016/j.apcata.2013.12.014>.

References

- [1] J.D. Murphy, J. Browne, E. Allen, C. Gallagher, Renew. Energy 55 (2013) 474.
- [2] H. Tolvanen, L. Kokko, R. Raiko, Fuel 111 (2013) 148–156.
- [3] E.S. Kim, S. Liu, M.M. Abu-Omar, N.S. Mosier, Energy Fuels 26 (2012) 1298–1304.
- [4] H. Kayser, C.R. Müller, C.A. García-González, I. Smirnova, W. Leitner, P.D. de María, Appl. Catal. A: Gen. 445–446 (2012) 180–186.
- [5] Z.H. Zhang, Z.K. Zhao, Carbohydr. Res. 344 (2009) 2069–2072.

Fig. 5. Time course of the aerobic oxidation of HMF into DFF at different reaction temperatures. (a) HMF conversion; (b) DFF yield. Reaction conditions: HMF (126 mg, 1 mmol) and Fe₃O₄/Mn₃O₄ (160 mg) were added into 7 mL of DMF, and the reactions were carried out at a set temperature with the flush of oxygen at a speed of 20 mL min⁻¹.



- [6] S. Al-Zuhair, M. Al-Hosany, Y. Zooba, A. Al-Hammadi, S. Al-Kaabi, *Renew. Energy* 56 (2013) 85–89.
- [7] T. Stauner, I.B. Silva, O.A. El Seoud, E. Frollini, D.F.S. Petri, *Cellulose* 20 (2013) 1109–1119.
- [8] R.J. van Putten, J.C. van der Waal, E. de Jong, C.B. Rasrendra, H.J. Heeres, J.G. de Vries, *Chem. Rev.* 113 (2013) 1499–1597.
- [9] Z.H. Zhang, Z.K. Zhao, *Bioresour. Technol.* 101 (2010) 1111–1114.
- [10] S. De, S. Dutta, A.K. Patra, B.S. Rana, A.K. Sinha, B. Saha, A. Bhaumik, *Appl. Catal. A: Gen.* 435–436 (2012) 197–203.
- [11] Z.H. Zhang, Q. Wang, H.B. Xie, W.J. Liu, Z.K. Zhao, *ChemSusChem* 4 (2011) 131–138.
- [12] N. Nikbin, S. Caratzoulas, D.G. VLachos, *ChemCatChem* 4 (2012) 504–511.
- [13] B. Liu, Z.H. Zhang, Z.K. Zhao, *Chem. Eng. J.* 215–216 (2013) 517–521.
- [14] X. Tong, Y. Ma, Y. Li, *Appl. Catal. A: Gen.* 385 (2010) 1–13.
- [15] J. Ma, Z. Du, J. Xu, Q. Chu, Y. Pang, *ChemSusChem* 4 (2011) 51–54.
- [16] K.T. Hopkins, W.D. Wilson, B.C. Bendan, D.R. McCurdy, J.E. Hall, R.R. Tidwell, A. Kumar, M. Bajic, D.W. Boykin, *J. Med. Chem.* 41 (1998) 3872–3878.
- [17] A. Gandini, *Green Chem.* 13 (2011) 1061–1083.
- [18] A.S. Amarasekara, D. Green, E. McMillan, *Catal. Commun.* 9 (2008) 286–288.
- [19] F.W. Lichtenthaler, *Acc. Chem. Res.* 35 (2002) 728–737.
- [20] L. Cottier, G. Descotes, J. Lewkowski, R. Skowroński, E. Viollet, *J. Heterocycl. Chem.* 32 (1995) 927–930.
- [21] J.F. Nie, J.H. Xie, H.C. Liu, *J. Catal.* 301 (2013) 83–91.
- [22] J.F. Nie, J.H. Xie, H.C. Liu, *Chin. J. Catal.* 34 (2013) 871–875.
- [23] C.A. Antonyraj, J. Jeong, B. Kim, S. Shin, S. Kim, K-Y. Lee, J.K. Cho, *J. Ind. Eng. Chem.* 19 (2013) 1056–1059.
- [24] A. Takagaki, M. Takahashi, S. Nishimura, K. Ebitani, *ACS Catal.* 1 (2011) 1562–1565.
- [25] N.-T. Le, P. Lakshmanan, K. Cho, Y. Han, H. Kim, *Appl. Catal. A: Gen.* 464–465 (2013) 305–312.
- [26] I. Sádaba, Y.Y. Gorbanov, S. Kegnæs, S.S.R. Putluru, R.W. Berg, A. Riisager, *Chem-CatChem* 5 (2013) 284–293.
- [27] M.J. Jin, D.H. Lee, *Angew. Chem. Int. Ed.* 49 (2010) 1119–1122.
- [28] H.Y. Sun, Q. Hua, F.F. Guo, Z.Y. Wang, W.X. Huang, *Adv. Synth. Catal.* 354 (2012) 569–573.
- [29] S.G. Wang, Z.H. Zhang, B. Liu, J.L. Li, *Catal. Sci. Technol.* 3 (2013) 2104–2112.
- [30] W.G. Fan, L. Gao, *J. Inorg. Mater.* 21 (2006) 789–794.
- [31] R. Song, S.H. Feng, H.J. Wang, C.M. Hou, *J. Solid State Chem.* 202 (2013) 57–60.
- [32] J. Lee, Y. Lee, J.K. Youn, H.B. Na, T. Yu, H. Kim, S.M. Lee, Y.M. Koo, J.H. Kwak, H.G. Park, H.N.M. Hwang, J.G. Park, J. Kim, T. Hyeon, *Small* 4 (2008) 143–152.
- [33] H. Zhang, C. Liang, Z. Tian, G. Wang, W. Cai, *J. Phys. Chem. C* 114 (2010) 12524–12528.
- [34] C. He, T. Sasaki, Y. Shimizu, N. Koshizaki, *Appl. Surf. Sci.* 254 (2008) 2196–2202.
- [35] A.M.E. Raj, S.G. Victoria, V.B. Jothy, C. Ravidhas, J. Wollschlager, M. Suerdorf, M. Neumann, M. Jayachandran, C. Sanjeeviraja, *Appl. Surf. Sci.* 256 (2010) 2920–2926.
- [36] G. Kataky, A. Ulman, M. Cojocaru, A. Gedanken, *J. Mater. Chem.* 9 (1999) 1501–1506.
- [37] K.R. Vuyyuru, P. Strasser, *Catal. Today* 195 (2012) 144–154.
- [38] S.K.R. Patil, C.R.F. Lund, *Energy Fuels* 25 (2011) 4745–4755.
- [39] E. Kang, D.W. Chae, B. Kim, Y.G. Kim, *J. Ind. Eng. Chem. Res.* 18 (2012) 174–177.
- [40] M. Biswal, V.V. Dhas, V.R. Mate, A. Banerjee, P. Pachfule, K.L. Agrawal, S.B. Ogale, C.V. Rode, *J. Phys. Chem. C* 115 (2011) 15440–15448.
- [41] V.V. Namboodiri, V. Polshettiwar, R.S. Varma, *Tetrahedron Lett.* 48 (2007) 8839–8842.
- [42] Z.Z. Yang, J. Deng, T. Pan, Q.X. Guo, Y. Fu, *Green Chem.* 14 (2012) 2986–2989.
- [43] M.D.D. Vigil, F.P. Delgado, V.C. Martinez, A.L. Ortiz, *Int. J. Chem. Reactor Eng.* 13 (2008) 1122–1128.
- [44] B. Saha, G. Dinesh, M.M. Abu-Omar, A. Modak, A. Bhaumik, *J. Catal.* 299 (2013) 316–320.